Published in final edited form as:
Nature. 2013 January 31; 493(7434): 679–683. doi:10.1038/nature11745.

Rag GTPase-mediated regulation of mTORC1 by nutrients is necessary for neonatal autophagy and survival

Alejo Efeyan[1,2,3,4,5], **Roberto Zoncu**[1,2,3,4,5], **Steven Chang**[1,2,3,4,5], **Iwona Gumper**[6], **Harriet Snitkin**[6], **Rachel L. Wolfson**[1,2,3,4,5], **Oktay Kirak**[1,7], **David D. Sabatini**[6], and **David M. Sabatini**[1,2,3,4,5,*]

[1]Whitehead Institute for Biomedical Research, Nine Cambridge Center, Cambridge, MA 02142, USA

[2]Broad Institute of Harvard and MIT, Seven Cambridge Center, Cambridge, Massachusetts 02142, USA

[3]Department of Biology, Massachusetts Institute of Technology (MIT), Cambridge, MA 02139, USA

[4]David H. Koch Institute for Integrative Cancer Research at MIT, 77 Massachusetts Avenue, Cambridge, MA 02139, USA

[5]Howard Hughes Medical Institute, MIT, Cambridge, MA, 02139

[6]Department of Cell Biology, New York University School of Medicine, New York, NY 10016-6497, USA

Abstract

The mTOR Complex 1 (mTORC1) pathway regulates organismal growth in response to many environmental cues, including nutrients and growth factors[1]. Cell-based studies showed that mTORC1 senses amino acids through the Rag family of GTPases [2,3], but their importance in mammalian physiology is unknown. Here, we generated knock-in mice that express a constitutively active form of RagA ($RagA^{GTP}$) from its endogenous promoter. $RagA^{GTP/GTP}$ mice develop normally, but fail to survive postnatal day 1. When delivered by Caesarian-section, fasted $RagA^{GTP/GTP}$ neonates die almost twice as rapidly as wild-type littermates. Within an hour of birth, wild-type neonates strongly inhibit mTORC1, which coincides with profound hypoglycaemia and a drop in plasma amino acid levels. In contrast, mTORC1 inhibition does not occur in $RagA^{GTP/GTP}$ neonates, despite identical reductions in blood nutrient levels. With prolonged fasting, wild-type neonates recover their plasma glucose levels, but $RagA^{GTP/GTP}$ mice remain hypoglycaemic until death, despite using glycogen at a faster rate. The glucose homeostasis defect correlates with the inability of fasted $RagA^{GTP/GTP}$ neonates to trigger

*correspondence: sabatini@wi.mit.edu.
[7]Present address: The Scripps Research Institute, 10550 North Torrey Pines Road, La Jolla, CA 92037

AUTHOR CONTRIBUTIONS

A.E. and D.M.S. conceived the project. A.E. designed and performed most experiments with input from D.M.S, and assistance from S.C., R.L.W. and O.K.. R.Z. performed experiments and participated in discussion of the results. I.G., H.S. and D.D.S. performed electron microscopy experiments and interpretations. D.D.S. helped with discussion and interpretation of results. A.E. wrote and D.M.S. edited the manuscript.

autophagy and produce amino acids for *de novo* glucose production. Because profound hypoglycaemia does not inhibit mTORC1 in $RagA^{GTP/GTP}$ neonates, we hypothesized that the Rag pathway signals glucose as well as amino acid sufficiency to mTORC1. Indeed, mTORC1 is resistant to glucose deprivation in $RagA^{GTP/GTP}$ fibroblasts, and glucose, like amino acids, controls its recruitment to the lysosomal surface, the site of mTORC1 activation. Thus, the Rag GTPases signal glucose and amino acid levels to mTORC1, and play an unexpectedly key role in neonates in autophagy induction and thus nutrient homeostasis and viability.

The mechanistic target of rapamycin (mTOR) is a serine-threonine kinase that as part of mTOR complex 1 (mTORC1) regulates anabolic and catabolic processes required for cell growth and proliferation [1]. mTORC1 integrates signals that reflect the nutritional status of an organism and senses growth factors and nutrients through distinct mechanisms. Growth factors regulate mTORC1 via the PI3K/Akt/TSC1-TSC2 axis, while amino acids act through the Rag family of GTPases [2,3]. When activated, these GTPases recruit mTORC1 to the lysosomal surface, an essential step in mTORC1 activation [3,4]. Amino acid levels regulate nucleotide binding to the Rag GTPases in a Ragulator- and vacuolar-type H^+-ATPase-dependent manner [4,5]. In the absence of amino acids, RagA (or RagB, which acts in an identical manner) is loaded with GDP, but becomes bound to GTP when amino acids are plentiful.

To study the physiological importance of the amino acid-dependent activation of mTORC1, we generated knock-in mice that express a constitutively active form of RagA. We chose to manipulate RagA because, although highly similar to RagB, RagA is much more abundant and widely expressed than RagB in mice (Supplementary Fig. 1a). By a single nucleotide substitution in the RagA coding sequence, we replaced glutamine in position 66 with leucine, generating a RagA mutant ($RagA^{Q66L}$) (Supplementary Fig. 1b) that is, regardless of amino acid levels, constitutively active, mimicking a permanent GTP-bound state [3,6] (hereafter referred to as $RagA^{GTP}$). We obtained mouse embryo fibroblasts (MEFs) from E13.5 embryos and evaluated mTORC1 signaling upon amino acid or serum deprivation. In $RagA^{+/+}$ and $RagA^{GTP/+}$ cells, deprivation of either amino acids (Fig. 1a) or serum (Supplementary Fig. 1c) suppressed mTORC1 activity, as determined by phosphorylation state of the mTORC1 substrates S6K1 and 4E-BP1. In contrast, in $RagA^{GTP/GTP}$ cells, mTORC1 activity was completely resistant to amino acid withdrawal (Fig. 1a). However, regulation of PI3K activity by serum was intact, as reflected by Akt phosphorylation (Supplementary Fig. 1c). Interestingly, RagA protein levels were reduced in $RagA^{GTP/GTP}$ cells, but this was not a consequence of lower $RagA^{GTP}$ mRNA expression (Fig. 1b), supporting the existence of a negative feedback triggered by RagA activity. Nevertheless, the cells show the expected amino acid-independent activation of mTORC1.

Cells lacking the TSC1-TSC2 tumor suppressor complex also have deregulated mTORC1 activity as such cells maintain mTORC1 signaling in the absence of growth factors [1]. Unlike TSC1- or TSC2-deficient MEFs[7,8], $RagA^{GTP/GTP}$ MEFs have normal proliferation rates without accelerated senescence (Supplementary Fig. 1d). Furthermore, unlike TSC1- or TSC2-deficient embryos, which die at E11.5-E13.5, $RagA^{GTP/GTP}$ embryos were indistinguishable from $RagA^{+/+}$ embryos (Supplementary Fig. 1e), and fetuses were

obtained and genotyped at term with the expected Mendelian ratios from heterozygous crosses. Thus, unlike with growth factor sensing, the inability of mTORC1 to sense amino acid deprivation does not compromise survival during embryonic development, with its steady placental supply of nutrients.

Although apparently not deleterious during *in utero* development, constitutive RagA activity greatly impairs early postnatal survival. Heterozygous $RagA^{GTP/+}$ mice did not have any obvious phenotypic alteration, in agreement with the normal signaling observed in $RagA^{GTP/+}$ MEFs. However, no $RagA^{GTP/GTP}$ mice were obtained at weaning, and were usually found dead within one day postpartum in breeding cages. Neonatal death can stem from a variety of defects, so we obtained full-term E19.5 mice by Caesarian-section and monitored them outside the breeding cage. Despite having a mild decrease in weight, $RagA^{GTP/GTP}$ neonates were barely distinguishable from control littermates (Fig. 1c, d), and histological analyses revealed no abnormalities (Supplementary Fig. 1f).

To understand how constitutive RagA activity affects the regulation of mTORC1 by fasting, we compared the phosphorylation levels of S6 and 4E-BP1, established markers of mTORC1 activity, in tissues obtained from neonates at birth or fasted for 1 or 10 hours. Interestingly, just 1 hour of fasting was sufficient to strongly inhibit mTORC1 in $RagA^{+/+}$ and $RagA^{GTP/+}$, but not $RagA^{GTP/GTP}$ neonates (Fig. 1e and Supplementary Fig. 1g), and this difference persisted even after 10 hours of fasting (Fig. 1f and Supplementary Fig. 1h). In contrast, Akt phosphorylation was modest at birth and decreased in mice of all genotypes (Supplementary Fig. 1g). As in MEFs, RagA protein levels were low in the tissues of $RagA^{GTP/GTP}$ mice, but this again was not due to reduced mRNA levels (Supplementary Fig. 1i). Collectively, these results indicate that constitutive RagA activity causes a profound defect in the response of mTORC1 to fasting.

To examine the consequences of this defect, we fasted neonates for longer periods of time, which revealed that $RagA^{GTP/GTP}$ neonates have an accelerated time to death (~14 hours for $RagA^{GTP/GTP}$ versus ~21 hours in $RagA^{+/+}$ and $RagA^{GTP/+}$) (Fig. 1g). This was not the consequence of unappreciated developmental defects, as the treatment of pups at birth with the mTORC1 inhibitor rapamycin, which suppressed mTORC1 activity in all neonates (Supplementary Fig. 1j), significantly delayed the death of fasted $RagA^{GTP/GTP}$ neonates from ~14 h to ~21 h; $p<0.01$) (Fig. 1h). These data suggest that Rag-mediated regulation of mTORC1 is necessary for mice to adapt to and survive the starvation period that they endure between birth and feeding.

Consistent with this notion, analysis of blood glucose levels revealed that fasted $RagA^{GTP/GTP}$ neonates suffer a profound defect in nutrient homeostasis. After one hour of fasting, glycaemia dropped dramatically in all neonates to below our 10 mg/dl limit of detection (Fig. 2a), but by 3 to 6 hours the wild-type animals restored their blood glucose to near birth levels (~40 mg/dl). In sharp contrast, in $RagA^{GTP/GTP}$ neonates, blood glucose levels never recovered and remained at ~10 mg/dl or lower until death (Fig. 2a). Consistent with its rescue of the accelerated lethality of the $RagA^{GTP/GTP}$ neonates during fasting (Fig. 1h), rapamycin administration partially reversed their defect in blood glucose levels (Fig.

2b). Moreover, injections of glucose prolonged the lifespan of fasted RagA$^{GTP/GTP}$ mice (Fig. 2c), arguing that a lack of glucose has a causal role in their compromised survival.

Because the inability to generate glucose from glycogen can cause perinatal lethality [9], we initially hypothesized that the RagA$^{GTP/GTP}$ neonates had a glycogen metabolism defect. However, RagA$^{GTP/GTP}$ neonates did not have defects in the protein or mRNA levels of the key enzymes of glycogen metabolism (Fig. 2d and Supplementary Fig. 2a). Moreover, at birth RagA$^{GTP/GTP}$ neonates had normal amounts of hepatic glycogen, which, upon fasting, they consumed at a faster rate than RagA$^{+/+}$ and RagA$^{GTP/+}$ animals (Fig. 2e), suggesting not a defect in its breakdown but rather accelerated use secondary to hypoglycaemia. Like with other characteristics of RagA$^{GTP/GTP}$ mice, rapamycin administration partially restored their hepatic glycogen (Fig. 2f).

We also considered defects in gluconeogenesis or the availability of gluconeogenic substrates as potential reasons for the inability of RagA$^{GTP/GTP}$ neonates to restore blood glucose levels upon fasting. Here too the RagA$^{GTP/GTP}$ neonates did not have aberrations in the expression levels of the relevant enzymes (Fig. 2d). However, after a 10-hour fast, RagA$^{GTP/GTP}$ neonates did have, compared to RagA$^{+/+}$ and RagA$^{GTP/+}$ littermates, significantly lower levels of plasma amino acids (Fig. 2g and Supplementary Fig. 2b). Because murine neonates are born without significant fat stores [10], lipid mobilization cannot serve as a substrate for *de novo* glucose production. Moreover, lactate, another substrate for gluconeogenesis, was not reduced in RagA$^{GTP/GTP}$ neonates (Supplementary Fig. 2c), arguing for a specific reduction in amino acid substrates. As with glucose levels and glycogen stores (Fig. 2b, f), rapamycin administration reversed the decrease in amino acids levels in RagA$^{GTP/GTP}$ neonates (Fig. 2g). Furthermore, injection of a mix of gluconeogenic amino acids, which can contribute to gluconeogenesis but not protein synthesis, delayed the onset of death of RagA$^{GTP/GTP}$ neonates (Fig. 2h), and injection of just alanine to fasted neonates provoked a significant increase in glycaemia (Supplementary Fig. 2d). These data are consistent with the glucose homeostasis defect of the fasted RagA$^{GTP/GTP}$ neonates being a consequence of reduced circulating amino acids, which leads to lower *de novo* glucose production and plasma levels, and accelerated death.

Several properties of the RagA$^{GTP/GTP}$ mice are reminiscent of autophagy-deficient mice [11,12], including the reduction in plasma amino acids and lifespan upon fasting, as well as the slightly lower birth weight. Although mTORC1 negatively regulates autophagy [13], and amino acids levels are regulators of autophagy in rats [14], many mTORC1-dependent and mTORC1-independent autophagy regulators exist [15]. Hence, we wondered if perturbing just one of the several inputs to mTORC1 could exert a dominant effect in the physiological regulation of autophagy.

Quantitative electron microscopic analyses of livers from one-hour fasted RagA$^{+/+}$ neonates revealed abundant autophagosomes, characterized by double limiting membranes (Fig. 3a and Supplementary Fig. 3a). Autophagosomes rapidly mature into single-membrane autophagolysosomes, so these were also found in RagA$^{+/+}$ livers (Fig. 3a and Supplementary Fig. 3a), albeit the ratio of autophagosomes to autophagolysosomes was high. Importantly, both autophagic vacuoles were rarely observed in fasted RagA$^{GTP/GTP}$

littermates (Fig. 3a). Similar results were obtained when skeletal muscle was analyzed (Fig. 3a).

Even after 10 hours of fasting, the autophagy defect in the livers of $RagA^{GTP/GTP}$ neonates persisted, as detected by the reduced cleavage of LC3B and degradation of p62 (Fig. 3b), which was increased by administration of rapamycin (Supplementary Fig. 3b). Biochemical analyses for these markers in skeletal and cardiac muscles from $RagA^{GTP/GTP}$ neonates after 1 and 2 h of fasting were also consistent with impaired autophagy (Fig. 3c). Cells in culture mirrored the *in vivo* findings (Fig. 3d), and these results were confirmed by detection of LC3B localization using fluorescence microscopy in amino acid-starved cells (Fig. 3e and Supplementary Fig. 3c). Consistently, phosphorylation of the autophagy activator ULK-1, a direct substrate of mTORC1 that was suppressed in $RagA^{+/+}$ MEFs upon amino acid withdrawal, remained high in $RagA^{GTP/GTP}$ cells (Fig. 3d). In addition, we looked at the transcription factor TFEB, which upregulates genes involved in lysosomal biogenesis and autophagy, but is excluded from the nucleus when phosphorylated by mTORC1[16,17]. Upon amino acid deprivation, TFEB localized to the nuclei of $RagA^{+/+}$ but not $RagA^{GTP/GTP}$ MEFs (Fig. 3f and Supplementary Fig. 3d). This result was mirrored by the decreased expression of TFEB transcriptional targets (Supplementary Fig 3d).

Serum withdrawal, which inhibits mTORC1 in a Rag-independent fashion, suppressed mTORC1 activity and triggered autophagy in MEFs of all genotypes (Supplementary Fig. 3e), indicating that constitutive RagA activity does not block autophagy induction by all signals. Thus, despite the multitude of pathways that regulate autophagy [15], Rag GTPase activity upstream of mTORC1 is a major regulator of autophagy *in vivo* during the perinatal period.

Maintenance of mTORC1 activity requires the simultaneous presence of growth factors, amino acids, and glucose [1]. We found that just one hour of fasting, both plasma amino acid and glucose levels were reduced in neonates of all genotypes (Fig. 2a and Supplementary Fig. 4a). The drop in nutrient levels correlated with a strong inhibition of mTORC1 activity in $RagA^{+/+}$ and $RagA^{GTP/+}$, but not $RagA^{GTP/GTP}$ neonates (Fig. 1e). Thus, despite a profound hypoglycaemic state, mTORC1 activity remained high in fasted $RagA^{GTP/GTP}$ neonates, a puzzling result given that the Rag GTPases are thought to have a specialized role in amino acid sensing. These observations led us to hypothesize that the Rag GTPases participate in the direct sensing of glucose levels, in addition to their established role in amino acid sensing. A well-established link between low glucose (but not amino acids [Supplementary Fig. 4b]) and mTORC1 inhibition is the AMP-activated protein kinase (AMPK). However, in MEFs lacking AMPK α1 and α2 (AMPK-DKO), mTORC1 activity was still repressed upon glucose deprivation, albeit less prominently than in wild-type MEFs (Fig. 4a). This indicates that an AMPK-independent pathway of mTORC1 inhibition exists, as shown recently in the context of metformin treatment [18]. Compared to control cells, mTORC1 signaling was largely resistant to glucose deprivation in $RagA^{GTP/GTP}$ MEFs (Fig. 4b and Supplementary Fig. 4c, e) and HEK-293T cells expressing $RagB^{GTP}$ (Supplementary Fig. 4d, e). It is unlikely that glucose indirectly inhibits mTORC1 by preventing amino acid transport, because amino acid esters, which freely enter cells and substitute for amino acids in mTORC1 activation [5], did not substitute for glucose (Supplementary Fig. 4f). Moreover,

intracellular amino acid levels were only marginally affected in cells deprived of glucose (Supplementary Fig. 4g). In addition, like AMPK-deficient cells [19,20], $RagA^{GTP/GTP}$ cells had enhanced sensitivity to long-term glucose deprivation-induced death (Fig. 4c). Constitutive RagA activity does not block AMPK action as aminoimidazole carboxamide ribonucleotide (AICAR), an AMPK activator, inhibited mTORC1 in cells of all genotypes (Supplementary Fig. 4h). In addition, AMPK activity, as monitored by acetyl-CoA carboxylase (ACC) phosphorylation, was induced to similar levels in glucose-deprived $RagA^{+/+}$ and $RagA^{GTP/GTP}$ cells (Fig. 4b and Supplementary Fig. 4c), but absent in AMPK-null cells (Fig. 4a). Another cellular nutrient sensor is GCN2 [21], but although it was regulated by amino acids, it was not by glucose; also, loss of GCN2 did not affect the inhibition of mTORC1 caused by amino acid or glucose starvation (Supplementary Fig. 4i).

Amino acids promote the Rag-dependent translocation of mTORC1 to the lysosomal surface, a necessary event for its activation [4]. Interestingly, glucose deprivation, like that of amino acids (Supplementary Fig. 4j), rendered mTORC1 diffusely localized in the cytoplasm of HEK-293T cells and, within minutes of glucose re-addition, mTORC1 re-clustered at lysosomes (Fig. 4d). However, in HEK-293T cells expressing $RagB^{GTP}$ and in $RagA^{GTP/GTP}$ MEFs, mTORC1 localized at the lysosomal surface regardless of glucose levels (Fig. 4d and Supplementary Fig. 4k). The lysosomal v-ATPase, necessary for the Rag-dependent activation of mTORC1 by amino acids, engages in amino acid-sensitive interactions with the Ragulator [5], and we found that glucose also regulates the binding of the v-ATPase to Ragulator (Fig. 4e), suggesting a shared regulatory mechanism. Finally, when amino acid and glucose concentrations at birth and after 1 hour neonatal fasting were reproduced in the *in vitro* culture medium, mTORC1 activity was suppressed in $RagA^{+/+}$ but not in $RagA^{GTP/GTP}$ cells placed under the one-hour fasting conditions (Fig. 4f). Hence, we propose that the Rag GTPases are a ‘multi-input nutrient sensor’, upon which amino acids and glucose converge, in a v-ATPase-dependent manner, upstream of mTORC1.

Altogether, our results support a chain of events that start with the interruption of maternal nutrient supply at birth, which inhibits mTORC1 presumably by converging negative inputs from profound hypoglycaemia and a drop in plasma amino acids, in a Rag-dependent fashion. During the period between birth and suckling, mTORC1 inhibition triggers autophagy, which generates the amino acids used to sustain plasma glucose levels via gluconeogenesis. Constitutive RagA activity prevents mTORC1 inhibition, leading to defective autophagy and, thus, insufficient amino acid production. The lower levels of gluconeogenic amino acids reduces hepatic generation of glucose, which accelerated glycogen breakdown fails to compensate, ultimately leading to hypoglycaemia, energetic exhaustion, and accelerated neonatal death (Fig. 4g). Thus, the Rag GTPases have a critical role in nutrient sensing by mTORC1 and in neonatal survival during fasting.

METHODS

Generation of $RagA^{GTP}$ mice

All animal work was performed in accordance with the Massachusetts Institute of Technology Committee on Animal Care. To target the RagA locus, we generated a construct consisting of a 4 Kbp 5′ homology arm upstream of the RagA gene, a transcriptional STOP

cassette containing a the hygromycin resistance gene, flanked by LoxP sites (loxP-PGK-Hyg-STOP-loxP)[22] placed at the 5′ end of the RagA exon, followed by a 3 Kbp 3′ homology arm downstream of RagA genomic sequence. For cloning purposes, a Not I restriction (GCGGCCGC) site was inserted into the 5′ homology arm, replacing the GGCGACGC sequence located 17 nucleotides upstream of the RagA ATG translation start codon. The LoxP-PGK-Hyg-STOP-loxP, previously cloned in the pMeca plasmid, was excised with Not I and inserted in the RagA construct. An A to T substitution in position +197 in RagA exon was performed by site-directed mutagenesis. This mutation translates into a Q66L amino acid substitution that renders a RagA protein that is constitutively active. See also Supplementary Fig. 1b. The construct was inserted into pPGKNeo.F2L2.DTA, linearized with Xma I and electroporated into male ES cells of mixed 129Sv/C57B6 background. ES colonies were picked and identified by Southern blot and confirmed by PCR amplification of specific insertion products. Positive ES cells clones were then injected into blastocysts and transferred into pseudo-pregnant females to obtain chimeric mice. Male chimeras were crossed to CMV-Cre transgenic females of C57BL/6J background, resulting in excision of the transcriptional STOP cassette and allowing expression of the $RagA^{Q66L}$ allele, and then intercrossed.

Preparation of MEFs

MEFs from E13.5 embryos of $RagA^{+/+}$, $RagA^{GTP/+}$ and $RagA^{GTP/GTP}$ genotype were prepared by chemical digestion followed by mechanical disaggregation. For spontaneous immortalization, MEFs were re-plated every 3 days until senescent. Spontaneously proliferating cells eventually arose after a senescent phase. AMPKα1/α2 DKO immortalized MEFs and matched wild-type MEFs were kindly provided by Rueben Shaw; David Ron kindly provided the GCN2 KO MEFs.

Amino acid, glucose and serum starvation and stimulation of cells

For amino acids and/or glucose deprivation in MEFs, sub-confluent cells were rinsed twice and incubated in RPMI without amino acids, glucose or both, and supplemented with 10% dialyzed FBS, as described [3]. Stimulation with glucose (5 mM) or amino acids (concentration as in RPMI) was performed for 10 min, unless otherwise indicated. For serum withdrawal, cells were rinsed twice in serum-free DMEM and incubated in serum-free DMEM for the indicated times; 100 nM was used for insulin stimulation. Aminoimidazole carboxamide ribonucleotide (AICAR, EMD Biosiences) was used at a final concentration of 2 mM. For cell survival experiments, cells were deprived of glucose or amino acids, and attached cells were counted 48 h later. For treatments with *in vivo* concentration of nutrients, MEFs were incubated with the following concentration of amino acids, reflecting the values found at birth (0 h) and after 1 h fasting (1 h) in control mice: (0 h: D: 34, T: 446, S: 268, N: 180, E: 194; Q: 1221, P: 289, G: 382, V: 321, C: 26, M: 245, I: 122, L: 192, Y: 165, F: 189, W: 124, K: 1026, H: 74, R: 199; 1 h: D: 48, T: 172, S: 82, N: 57, E: 128, Q: 592, P: 183, G: 298, V: 154, C: 17, M: 164, I: 26, L: 37, Y: 71, F: 72, W: 92, K: 723, H: 30, R: 78, all in μM. Similarly, the concentrations of glucose were 0 h: 45 mg/dl and 1 h: 12 mg/dl. Protein extracts were obtained as above.

Immunoblotting

Reagents were obtained from the following sources: anti phospho-T389 S6K1, phospho-S240/244 S6, phospho-T37/T46 4E-BP1, phosho-T308 Akt, phospho-S473 Akt, phospho-S757 ULK1, phospho-S9 GSK3-β, phospho-S641 glycogen synthase, phospho-S51-eIF2a; total Akt, S6K1, 4E-BP1, GSK3-β, glycogen synthase and eIF2a from Cell Signaling Technology (CST); anti LC3B from CST and Novus Biologicals; anti β-actin (clone AC-15) from Sigma; anti p62 from America Research Products, CST and Enzo Life Sciences; anti PYGL from Santa Cruz. Cells were rinsed once with ice-cold PBS and lysed in ice-cold lysis buffer (50 mM HEPES [pH 7.4], 40 mM NaCl, 2 mM EDTA, 1.5 mM sodium orthovanadate, 50 mM NaF, 10 mM pyrophosphate, 10 mM glycerophosphate, and 1% Triton X-100, and one tablet of EDTA-free complete protease inhibitors [Roche] per 25 ml). Cell lysates were cleared by centrifugation at 13,000 rpm for 10 min. Proteins extracts were denatured by the addition of sample buffer, boiled for 5 min, resolved by SDS-PAGE, and analyzed by immunoblotting.

Immunofluorescence assays in cells

MEFs or HEK-293T cells were plated on fibronectin-coated 2 cm^2 glass coverslips at a density of 50–100,000 cells/coverslip. For overexpression of GFP-LC3B and TFEB-GFP, cells were transfected by nucleofection (Lonza) using 1μg for 2×10^6 cells. The following day, cells were transferred to amino acid- or glucose-free RPMI, starved for 60 min or starved for 50 min and re-stimulated for 10 min with amino acids or glucose, rinsed with cold PBS once and fixed for 15 min with 4% paraformaldehyde. Coverslips were permeabilized with 0.05% Triton X-100 in PBS and then incubated with primary antibodies in 5% normal donkey serum for 1 h, rinsed, and incubated with Alexa fluor-conjugated secondary antibodies (Invitrogen) diluted 1:400, for 45 min. Cells overexpressing GFP-LC3B and TFEB-GFP were fixed in 4% paraformaldehyde, rinsed and imaged. Coverslips were mounted on glass slides using Vectashield (Vector Laboratories) and imaged on a spinning disk confocal system (Perkin Elmer) equipped with 405 nm, 488 nm and 561 nm laser lines, through a 63X objective.

Co-immunoprecipitation assays

HEK-293T cells stably expressing FLAG-tagged proteins were processed as described [5].

Quantitative PCR

Total RNA was extracted with RNAesy (Qiagen), retro-transcribed with Superscript III (Invitrogen) and used at 1:100 dilution in quantitative real time PCR in an Applied Biosystems thermocycler. 36B4 and β-actin were for normalization. The following primers were used:

RagA F	GAACCTGGTGCTGAACCTGT
RagA R	GATGGCTTCCAGACACGATT
RagB F	TTCGATTTCTGGGAAACCTG

RagB R	AGTTCACGGCTCTCCACATC
mTOR F	GGTGCTGACCGAAATGAGGG
mTOR R	TCTTGCCCTTGTGTTCTGCA
Raptor F	TGGCAGCCAAGGGCTCGGTA
Raptor R	GCAGCAGCTCGTGTGCCTCA
Rictor F	TCGCAACTCACCACAAGCGGG
Rictor R	TGCAAGCATCTGTGGCTGCCG
Pepck F	CGATGACATCGCCTGGATGA
Pepck R	TCTTGCCCTTGTGTTCTGCA
G-6-P F	GAAGGCCAAGAGATGGTGTGA
G-6-P R	TGCAGCTCTTGCGGTACATG
Glucokinase F	GAGATGGATGTGGTGGCAAT
Glucokinase R	ACCAGCTCCACATTCTGCAT
36B4 F	TAAAGACTGGAGACAAGGTG
36B4 R	GTGTACTCAGTCTCCACAGA
SQSTM1 F	GAACTCGCTATAAGTGCAGTGT
SQSTM1 R	AGAGAAGCTATCAGAGAGGTGG
Vps11 F	GGAGCCTGGTCTTTGGAGA
Vps11 R	GCTGTAGAGAACGTGGCAAGA
Vps33a F	TCTGTGCTCAGCAAGAAGGCGA
Vps33a R	GGACGCAAACTGCTTGATCTCC
Vps8 F	GATGGACCATCTCCTGAAACAGG
Vps8 R	AGCCTTCCTCTTGCTGACATCC
UVRag F	GGAATAATGCCGGATCGTCTG
UVRag R	CCTTTCCACCCCAAATCTTCAC
Actin F	GGCACCACACCTTCTACAATG
Actin R	GTGGTGGTGAAGCTGTAGCC

Neonatal fasting and treatments

E17.5 and E18.5 pregnant females were injected with 2 mg progesterone (Sigma-Aldrich) to prevent early delivery. At E19.5, females were euthanized and fetuses immediately obtained by C-section. Successfully resuscitated neonates were placed in a humidified chamber at 30°C and fasted. Rapamycin (LC Laboratories, Woburn, MA) was administered intraperitoneally at a volume of 100 μl (1 mg/ml concentration) to pregnant females 4 hours before C-section, and neonates were injected subcutaneous (s.c.) with 5 μl immediately after C-section. 30% glucose in PBS or with gluconeogenic amino acids mix (A: 500 mg/ml; N: 10 mg/ml; S: 6 mg/ml; D, E and P: 4 mg/ml; G: 2 mg/ml) in PBS were injected s.c. every 3–6 hours.

Electron microscopy

Tissues were obtained and immediately fixed in 2% glutaraldehyde in 0.1 M sodium cacodylate buffer pH7.4 at room temperature. After post-fixation in 2% OsO_4 blocks were

processed for embedding in Epon 812. Thin sections were obtained, stained with uranyl acetate and lead citrate, and examined by TEM in a JEOL EX 1200 electron microscope.

Measurement of glucose and amino acid levels

Blood glucose was quantified with a glucometer and glucose test strips (Bayer Contour), with a lower detection limit of 10 mg/dl. For amino acid quantification, plasma was analyzed using the Waters (Milford, MA) MassTrak Amino Acid system. Pre-column derivatization of amino acids via molar excess of 6-aminoquinolyl-N-hydroxysuccinimidyl carbamate was performed, converting both primary and secondary amino acids to stable chromophores. The derivatized amino acids are separated and detected using an Aquity UPLC system (Waters, Milford, MA) and UV absorbance. Amino acid levels in MEFs were quantified in the same manner after total extraction in boiling dH_2O.

Hepatic glycogen content measurement

Glycogen was measured in liver samples as described [23]. Briefly, glycogen was extracted from neonatal livers in 30% KOH saturated with Na_2SO_4, precipitated in 95% ethanol and re-suspended in ddH_2O. After addition of phenol and H_2SO_4, absorbance at 490 nm was measured in triplicates.

Statistical analyses

For Kaplan-Meier survival curves, comparisons were made with the Log-rank Mantel-Cox method. For qtPCR analyses, measurements of glycaemia, plasma amino acids and glycogen content, non-parametric t-tests were performed. Chi-squared tests were also performed for the effects of rapamycin on glycaemia.

Supplementary Material

Refer to Web version on PubMed Central for supplementary material.

Acknowledgments

We thank members of the Sabatini Lab for helpful suggestions, and Amanda Hutchins for technical assistance. We thank Reuben Shaw for providing the AMPK-DKO MEFs, David Ron for the GCN2-KO MEFs, and Mariano Barbacid for the transcriptional STOP cassette. Supported by grants from the National Institutes of Health (R01 CA129105, R01 CA103866 and R37 AI047389) and awards from the American Federation for Aging, Starr Foundation, Koch Institute Frontier Research Program, and the Ellison Medical Foundation to D.M.S., and fellowships from the Human Frontiers Science Program to A.E., and the Jane Coffin Childs Memorial Fund for Medical Research and the LAM Foundation to R.Z. D.M.S. in an investigator of Howard Hughes Medical Institute.

References

1. Zoncu R, Efeyan A, Sabatini DM. mTOR: from growth signal integration to cancer, diabetes and ageing. Nat Rev Mol Cell Biol. 2010; 12:21–35. nrm3025 [pii]. 10.1038/nrm3025 [PubMed: 21157483]
2. Kim E, Goraksha-Hicks P, Li L, Neufeld TP, Guan KL. Regulation of TORC1 by Rag GTPases in nutrient response. Nat Cell Biol. 2008; 10:935–945. ncb1753 [pii]. 10.1038/ncb1753 [PubMed: 18604198]
3. Sancak Y, et al. The Rag GTPases bind raptor and mediate amino acid signaling to mTORC1. Science. 2008; 320:1496–1501. 1157535 [pii]. 10.1126/science.1157535 [PubMed: 18497260]

4. Sancak Y, et al. Ragulator-Rag complex targets mTORC1 to the lysosomal surface and is necessary for its activation by amino acids. Cell. 2010; 141:290–303. S0092-8674(10)00177-7 [pii]. 10.1016/j.cell.2010.02.024 [PubMed: 20381137]
5. Zoncu R, et al. mTORC1 senses lysosomal amino acids through an inside-out mechanism that requires the vacuolar H-ATPase. Science. 2011; 334:678–683. 334/6056/678 [pii]. 10.1126/science.1207056 [PubMed: 22053050]
6. Hirose E, Nakashima N, Sekiguchi T, Nishimoto T. RagA is a functional homologue of S. cerevisiae Gtr1p involved in the Ran/Gsp1-GTPase pathway. J Cell Sci. 1998; 111 (Pt 1):11–21. [PubMed: 9394008]
7. Kwiatkowski DJ, et al. A mouse model of TSC1 reveals sex-dependent lethality from liver hemangiomas, and up-regulation of p70S6 kinase activity in Tsc1 null cells. Hum Mol Genet. 2002; 11:525–534. [PubMed: 11875047]
8. Zhang H, et al. Loss of Tsc1/Tsc2 activates mTOR and disrupts PI3K-Akt signaling through downregulation of PDGFR. J Clin Invest. 2003; 112:1223–1233. 112/8/1223 [pii]. 10.1172/JCI17222 [PubMed: 14561707]
9. Scheuner D, et al. Translational control is required for the unfolded protein response and in vivo glucose homeostasis. Mol Cell. 2001; 7:1165–1176. S1097-2765(01)00265-9 [pii]. [PubMed: 11430820]
10. Birsoy K, et al. Analysis of gene networks in white adipose tissue development reveals a role for ETS2 in adipogenesis. Development. 2011; 138:4709–4719. 138/21/4709 [pii]. 10.1242/dev.067710 [PubMed: 21989915]
11. Kuma A, et al. The role of autophagy during the early neonatal starvation period. Nature. 2004; 432:1032–1036. nature03029 [pii]. 10.1038/nature03029 [PubMed: 15525940]
12. Komatsu M, et al. Impairment of starvation-induced and constitutive autophagy in Atg7-deficient mice. J Cell Biol. 2005; 169:425–434. jcb.200412022 [pii]. 10.1083/jcb.200412022 [PubMed: 15866887]
13. Mizushima N, Levine B, Cuervo AM, Klionsky DJ. Autophagy fights disease through cellular self-digestion. Nature. 2008; 451:1069–1075. nature06639 [pii]. 10.1038/nature06639 [PubMed: 18305538]
14. Mortimore GE, Schworer CM. Induction of autophagy by amino-acid deprivation in perfused rat liver. Nature. 1977; 270:174–176. [PubMed: 927529]
15. Kroemer G, Marino G, Levine B. Autophagy and the integrated stress response. Mol Cell. 2010; 40:280–293. S1097-2765(10)00751-3 [pii]. 10.1016/j.molcel.2010.09.023 [PubMed: 20965422]
16. Roczniak-Ferguson A, et al. The Transcription Factor TFEB Links mTORC1 Signaling to Transcriptional Control of Lysosome Homeostasis. Science signaling. 2012; 5:ra42.10.1126/scisignal.2002790 [PubMed: 22692423]
17. Settembre C, et al. *A* lysosome-to-nucleus signalling mechanism senses and regulates the lysosome via mTOR and TFEB. EMBOJ. 2012 emboj201232 [pii]. 10.1038/emboj.2012.32
18. Kalender A, et al. Metformin, independent of AMPK, inhibits mTORC1 in a rag GTPase-dependent manner. Cell Metab. 2010; 11:390–401. S1550-4131(10)00084-7 [pii]. 10.1016/j.cmet.2010.03.014 [PubMed: 20444419]
19. Choo AY, et al. Glucose addiction of TSC null cells is caused by failed mTORC1-dependent balancing of metabolic demand with supply. Mol Cell. 2010; 38:487–499. S1097–2765(10)00369-2 [pii]. 10.1016/j.molcel.2010.05.007 [PubMed: 20513425]
20. Shaw RJ, et al. The tumor suppressor LKB1 kinase directly activates AMP- activated kinase and regulates apoptosis in response to energy stress. Proc Natl Acad Sci USA. 2004; 101:3329–3335. 0308061100 [pii]. 10.1073/pnas.0308061100 [PubMed: 14985505]
21. Proud CG. eIF2 and the control of cell physiology. Semin Cell Dev Biol. 2005; 16:3–12.10.1016/j.semcdb.2004.11.004 [PubMed: 15659334]
22. Guerra C, et al. Tumor induction by an endogenous K-ras oncogene is highly dependent on cellular context. Cancer Cell. 2003; 4:111–120. S1535610803001910 [pii]. [PubMed: 12957286]
23. Lo S, Russell JC, Taylor AW. Determination of glycogen in small tissue *samples*. J Appl Physiol. 1970; 28:234–236. [PubMed: 5413312]

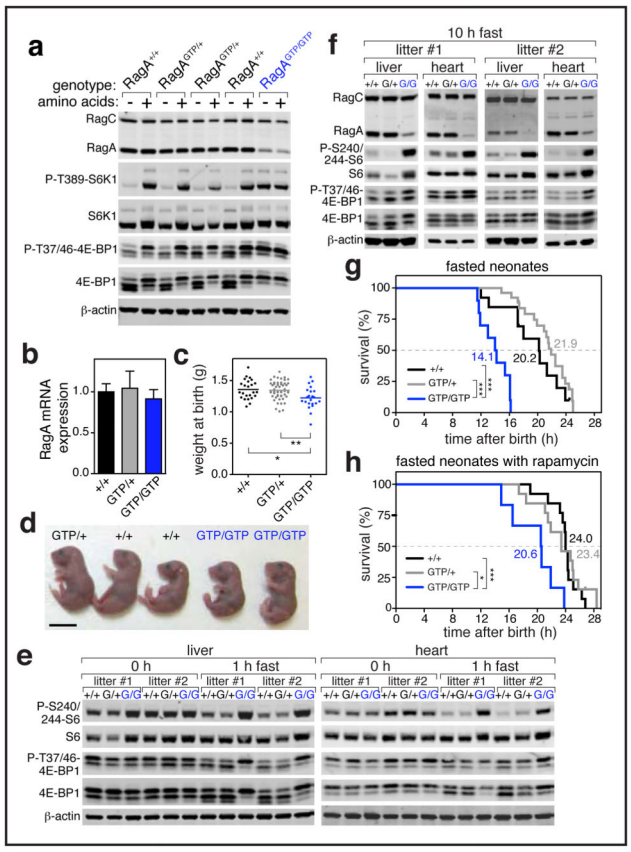

Figure 1. Characterization of RagA$^{GTP/GTP}$ mice

(A) Mouse embryo fibroblasts (MEFs) of RagA$^{+/+}$, RagA$^{GTP/+}$ and RagA$^{GTP/GTP}$ genotypes were deprived of amino acids for 1 h and re-stimulated for 10 min. Whole cell protein lysates were immunoblotted for indicated proteins. **(B)** Total RNA was extracted from RagA$^{+/+}$ (n=3), RagA$^{GTP/+}$ (n=3), and RagA$^{GTP/GTP}$ (n=2) MEFs and RagA mRNA expression determined by qPCR (mean ± SEM). **(C)** Weights of RagA$^{+/+}$ (n=24), RagA$^{GTP/+}$ (n=52), and RagA$^{GTP/GTP}$ (n=22) mice at birth (data are scatter dots, mean ± SD). **(D)** Representative photos of RagA$^{+/+}$, RagA$^{GTP/+}$, and RagA$^{GTP/GTP}$ neonates. Bar indicates 1 cm. **(E)** Early suppression of mTORC1 signaling after birth was determined by immunoblotting of protein extracts from liver and heart of RagA$^{+/+}$ (+/+), RagA$^{GTP/+}$ (G/+), and RagA$^{GTP/GTP}$ (G/G) neonates immediately after C-section (0 h) or after 1 h of fasting (1 h fast). **(F)** Liver and heart extracts from 10 h-fasted RagA$^{+/+}$, RagA$^{GTP/+}$, and RagA$^{GTP/GTP}$ neonates were analyzed by immunoblotting for the indicated proteins. **(G)** Survival curve of fasted neonates. Neonates obtained by C-section and resuscitated were fasted and their survival monitored (+/+: n=13; G/+: n=26; G/G: n=10). **(H)** Survival curve of fasted neonates treated with rapamycin. Neonates obtained by C-section and resuscitated were fasted and their survival monitored (untreated: n=10, rapamycin: n=6). Numbers indicate the median survival for each curve. *: p<0.05; **: p<0.01; ***: p<0.005.

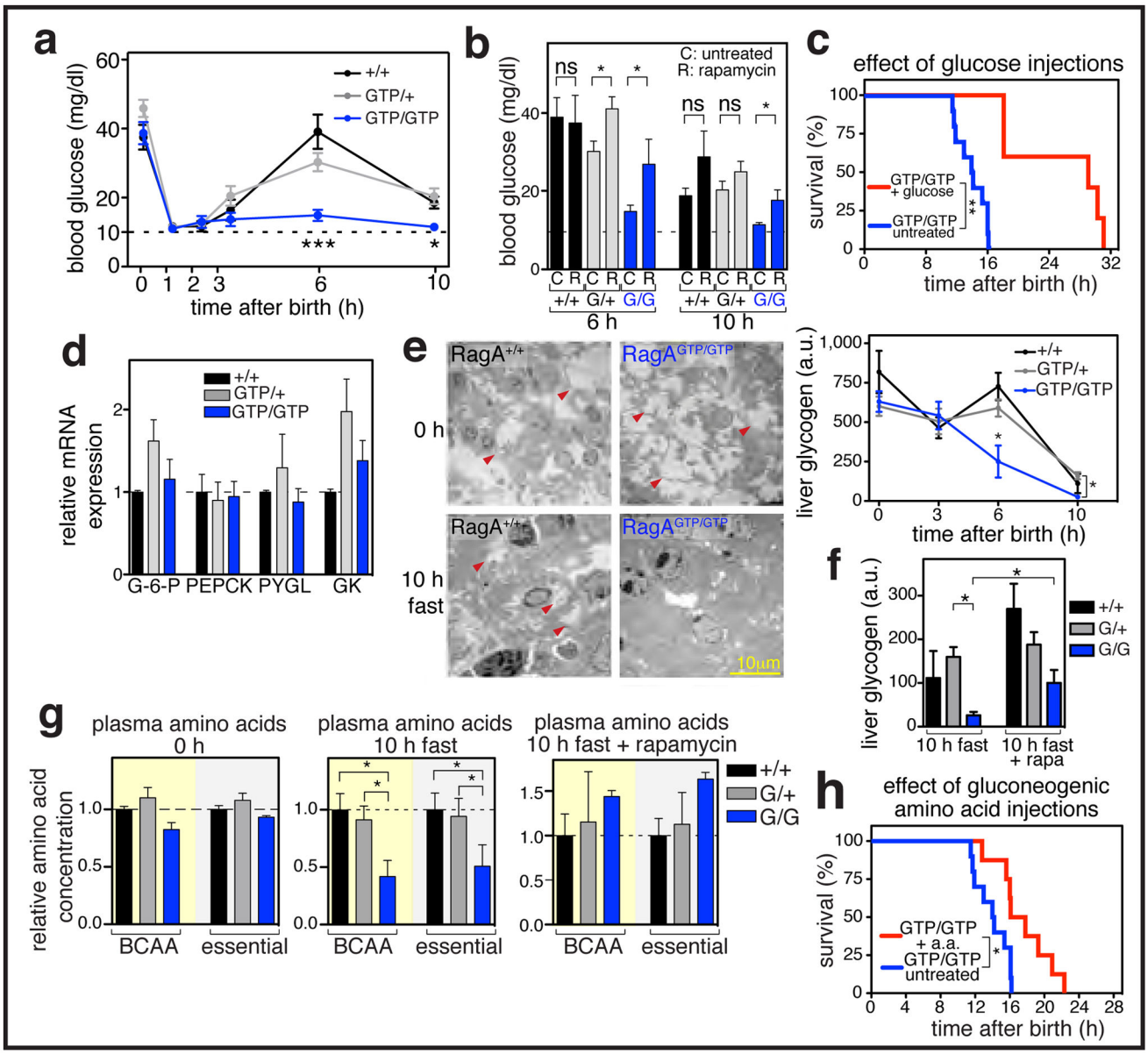

Figure 2. Profound glucose homeostasis defect in RagA$^{GTP/GTP}$ mice

(A) Glycaemia drop in RagA$^{+/+}$, RagA$^{GTP/+}$ and RagA$^{GTP/GTP}$ and recovery in fasted RagA$^{+/+}$ and RagA$^{GTP/+}$ but not in RagA$^{GTP/GTP}$ neonates (+/+: n=5, 18, 4, 5, 9, 8; G/+: n=10, 26, 10, 13, 26, 21; G/G: n=7, 20, 9, 10, 16, 11, for 0, 1, 2, 3, 6 and 10 h, respectively; mean ± SEM). **(B)** Rapamycin significantly increases glycaemia in 6 h- and 10 h-fasted RagA$^{GTP/GTP}$ (mean ± SEM). **(C)** Extension of survival by glucose injections in fasted RagA$^{GTP/GTP}$ neonates (untreated: n=10; glucose: n=5). **(D)** Normal expression of genes involved in glucose metabolism in neonatal liver (+/+: n=2, G/+: n=5; G/G: n=4, mean ± SEM). **(E)** Left: Representative electron microscopy images showing abundant glycogen content in RagA$^{+/+}$ and RagA$^{GTP/GTP}$ hepatocytes before fasting (0 h, upper panels) and more pronounced glycogen depletion after 10 h of fasting (lower panels) in RagA$^{GTP/GTP}$ neonates. Right: Quantification of hepatic glycogen content (+/+: n=5, 3, 4, 4; G/+: n=11, 7, 14, 15; G/G: n=6, 4, 4, 6; for 0, 1, 3, 6 and 10 h, respectively; mean ± SEM). **(F)** Partial rescue of hepatic glycogen content in 10 h-fasted RagA$^{GTP/GTP}$ neonates treated with rapamycin (mean ± SEM). **(G)** Quantification of neonatal plasma levels of branched-chain (BCAA) and essential

amino acids at birth (left), after 10 h fasting (middle), and after 10 h fasting with rapamycin treatment (right) (n for +/+, G/+ and G/G, respectively: n=4, 5 and 4 for 0 h; n=4, 4 and 3 for 10 h; n=2, 5 and 3 for rapamycin; mean ± SD). Values are expressed relative to $RagA^{+/+}$ levels at each time point. **(H)** Extension of survival by injection of a combination of gluconeogenic amino acids in fasted $RagA^{GTP/GTP}$ neonates (untreated: n=10; amino acids: n=8). *: $p<0.05$; **: $p<0.01$; ns: $p>0.05$.

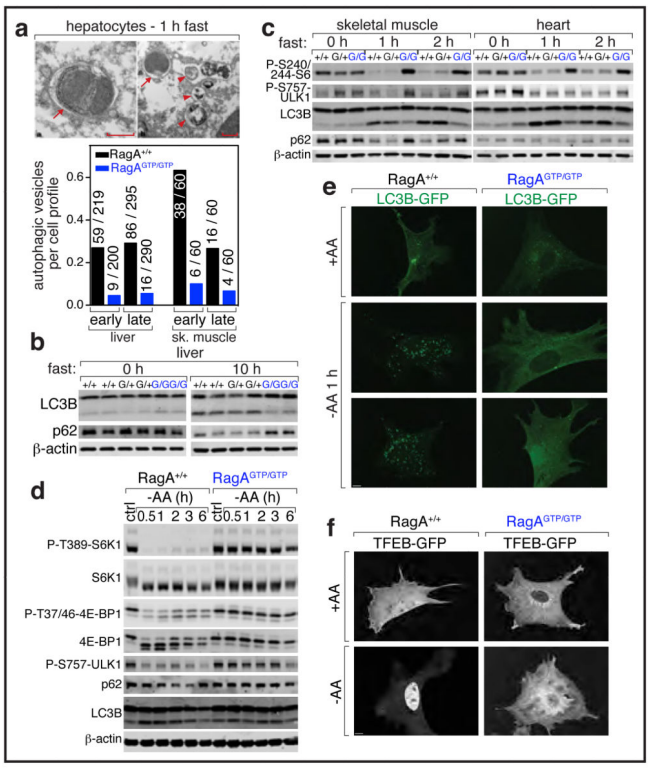

Figure 3. Impaired autophagy in RagA$^{GTP/GTP}$ neonates

(A) Top: Representative micrographs of autophagosomes and autophagolysosomes in hepatocytes from 1 h fasted RagA$^{+/+}$ neonates. Typical autophagosome with a double limiting membrane (arrows); autophagosome and several autolysosomes (arrowheads). Bar indicates 5 μm. Bottom: Frequency of the two types of organelles (early: autophagosomes; late: autophagolysosomes) detected in cell profiles of hepatocytes and skeletal myocytes from RagA$^{+/+}$ and RagA$^{GTP/GTP}$ neonates. **(B)** Protein extracts from livers of neonates at C-section (0 h) and 10 h-fasted (10 h) were immunblotted for autophagy markers LC3B and p62. **(C)** Protein extracts from skeletal muscle and heart from neonates at C-section (0 h), 1 h- and 2 h-fasted, were immunoblotted for indicated proteins. **(D)** Triggering of autophagy by amino acid withdrawal in MEFs. MEFs were deprived of amino acids for the indicated time points, whole cell protein extracts were obtained and mTORC1 activity and autophagic activity determined by immunoblotting. **(E)** Recombinant LC3B-GFP was expressed in RagA$^{+/+}$ and RagA$^{GTP/GTP}$ MEFs and LC3B localization, in the presence and absence of amino acids, monitored by fluorescence microscopy. LC3B-GFP clustering, indicative of autophagy, was observed in amino acid-starved RagA$^{+/+}$ but not RagA$^{GTP/GTP}$ MEFs. Bar indicates 10 μm. **(F)** Localization of recombinant TFEB-GFP was determined in MEFs as in (E). Nuclear (active) TFEB was observed in RagA$^{+/+}$ MEFs upon amino acid withdrawal.

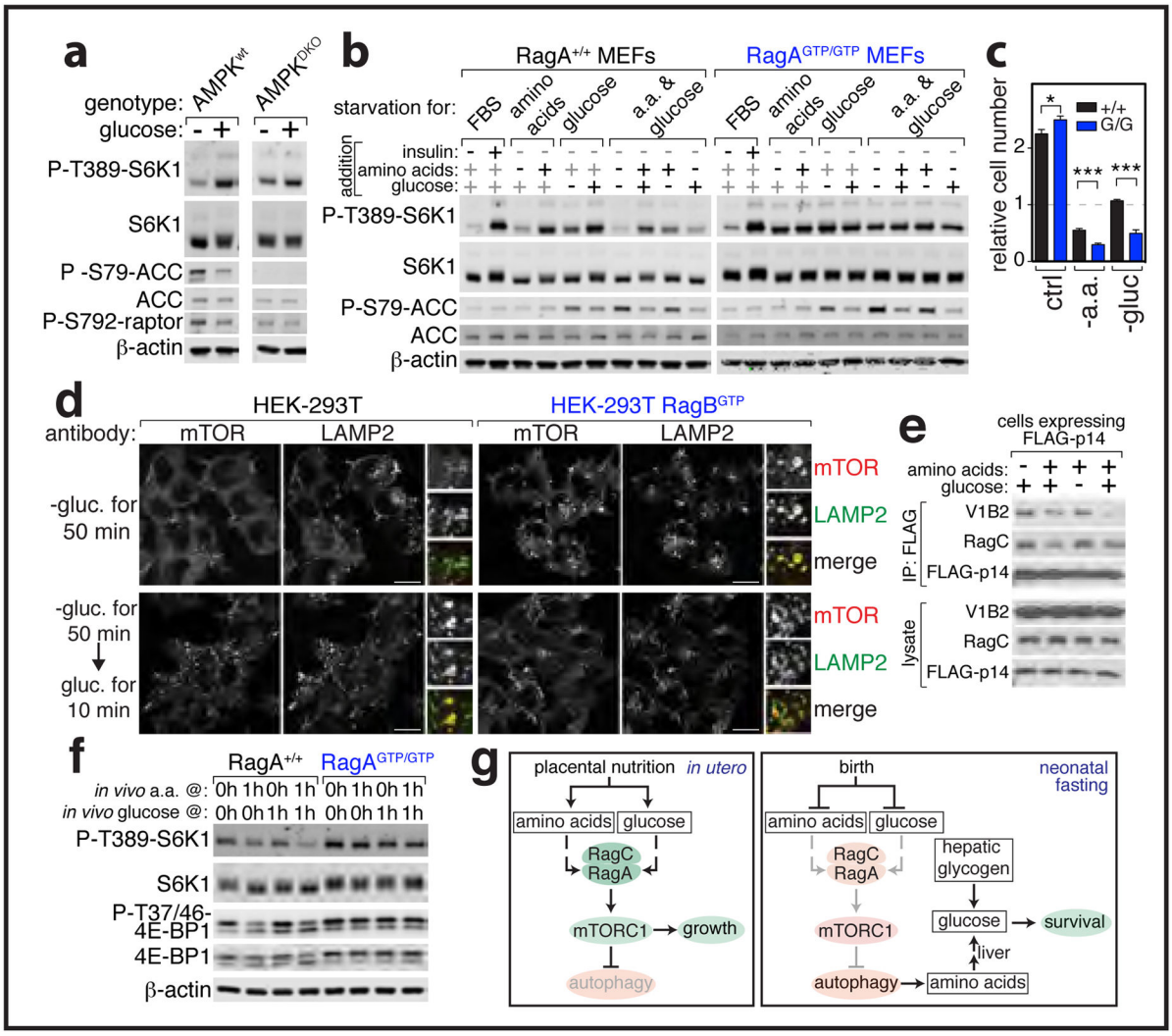

Figure 4. The Rag GTPases mediate inhibition of mTORC1 by glucose deprivation

(A) AMPKα1/α2 double knock-out (DKO) and wt MEFs were deprived of glucose for 1 h and re-stimulated for 10 min. Whole cell extracts were immunoblotted for the indicated proteins. **(B)** Immortalized MEFs of the indicated genotypes were deprived of growth factors, glucose, amino acids, or glucose and amino acids for 1 h and re-stimulated with glucose and/or amino acids for 10 min. Whole cell lysates were immunoblotted for the indicated proteins. **(C)** $RagA^{+/+}$ and $RagA^{GTP/GTP}$ immortalized MEFs were deprived of glucose or amino acids and surviving cells quantified in triplicate after 48 h. Cell number is indicated relative to cell number at the start of the treatment; mean ± SD; ***: $p<0.005$. **(D)** mTOR localization as detected by immunofluorescence. In HEK-293T cells, glucose deprivation causes mTOR to localize to diffuse small puncta throughout the cytoplasm. Re-addition of glucose leads to mTOR shuttling to the lysosomal surface, co-localizing with the lysosomal protein Lamp2. HEK-293T-$RagB^{GTP}$ cells show mTOR localized at the lysosomal surface, regardless of glucose levels. Bar indicates 10 μm. **(E)** Glucose and amino acids affect the binding of the v-ATPase to the Ragulator complex. HEK-293T expressing FLAG-p14 were deprived of glucose or amino acids for 90 min and re-stimulated for 20 min. Protein extracts and immunoprecipitates were immunoblotted for the indicated proteins. **(F)** $RagA^{+/+}$ and $RagA^{GTP/GTP}$ primary MEFs were cultured for 1 h in media with the glucose and amino acid concentrations measured in neonates at birth (0 h) or after 1 h fasting

(1 h) and whole cells protein extracts were analyzed by immunoblotting. **(G)** Speculative model for constitutive RagA-induced neonatal lethality. Green and red boxes indicate active and inactive protein or process, respectively.